SINTEF
PROCEEDINGS
2

Proceedings of the 12th International Conference on Computational Fluid Dynamics in the Oil & Gas, Metallurgical and Process Industries

Progress in Applied CFD – CFD2017

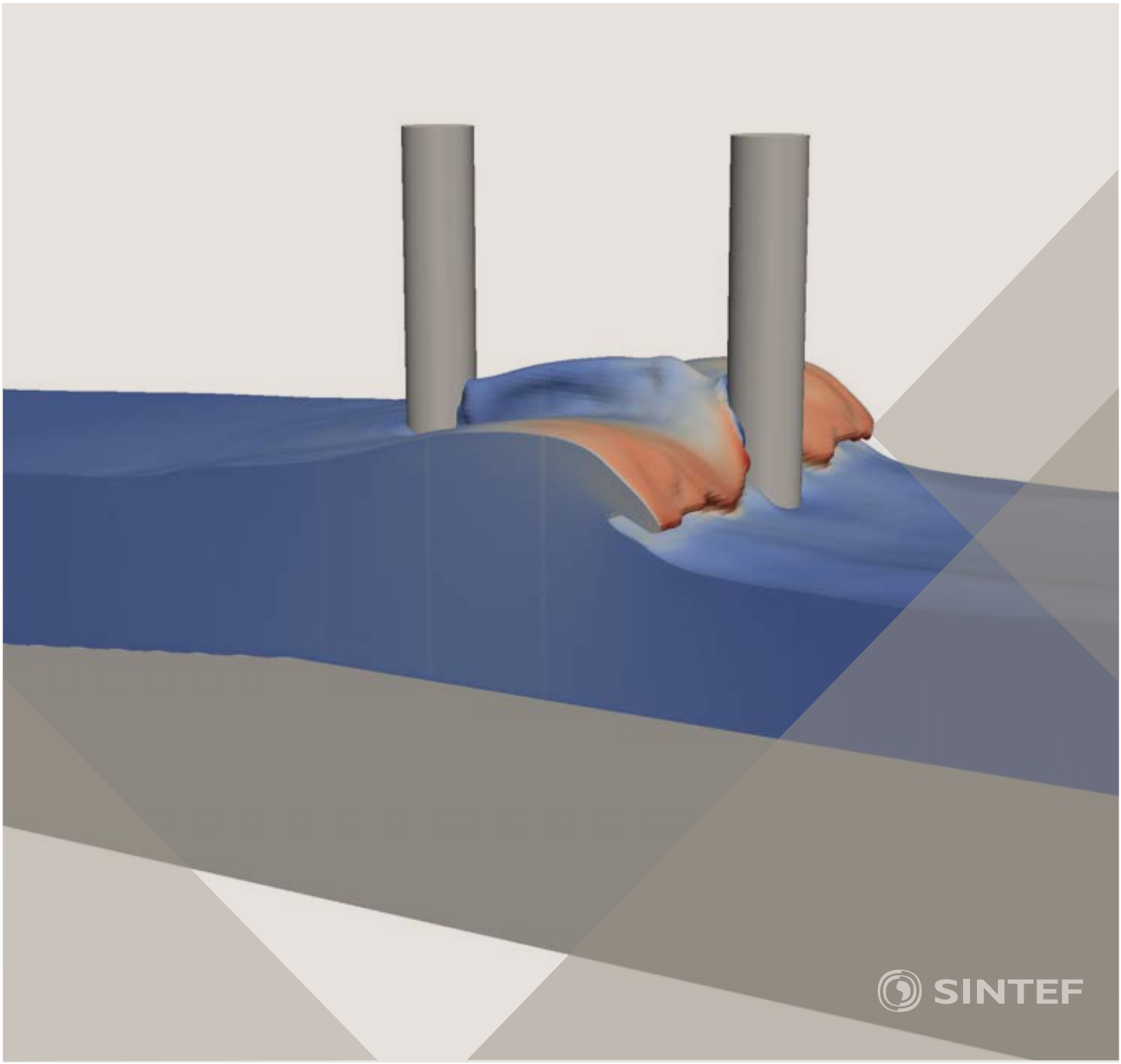

SINTEF Proceedings

Editors:
Jan Erik Olsen and Stein Tore Johansen

Progress in Applied CFD – CFD2017

Proceedings of the 12th International Conference on Computational Fluid Dynamics in the Oil & Gas, Metallurgical and Process Industries

SINTEF Academic Press

SINTEF Proceedings no 2
Editors: Jan Erik Olsen and Stein Tore Johansen
Progress in Applied CFD – CFD2017
Selected papers from 10th International Conference on Computational Fluid Dynamics in the Oil & Gas, Metallurgical and Process Industries

Key words:
CFD, Flow, Modelling

Cover, illustration: Arun Kamath

ISSN 2387-4295 (online)
ISBN 978-82-536-1544-8 (pdf)

SINTEF Academic Press
Address: Forskningsveien 3 B
PO Box 124 Blindern
N-0314 OSLO
Tel: +47 73 59 30 00
Fax: +47 22 96 55 08

www.sintef.no/byggforsk
www.sintefbok.no

SINTEF Proceedings
SINTEF Proceedings is a serial publication for peer-reviewed conference proceedings on a variety of scientific topics.
The processes of peer-reviewing of papers published in SINTEF Proceedings are administered by the conference organizers and proceedings editors. Detailed procedures will vary according to custom and practice in each scientific community.

PREFACE

This book contains all manuscripts approved by the reviewers and the organizing committee of the 12th International Conference on Computational Fluid Dynamics in the Oil & Gas, Metallurgical and Process Industries. The conference was hosted by SINTEF in Trondheim in May/June 2017 and is also known as CFD2017 for short. The conference series was initiated by CSIRO and Phil Schwarz in 1997. So far the conference has been alternating between CSIRO in Melbourne and SINTEF in Trondheim. The conferences focuses on the application of CFD in the oil and gas industries, metal production, mineral processing, power generation, chemicals and other process industries. In addition pragmatic modelling concepts and bio-mechanical applications have become an important part of the conference. The papers in this book demonstrate the current progress in applied CFD.

The conference papers undergo a review process involving two experts. Only papers accepted by the reviewers are included in the proceedings. 108 contributions were presented at the conference together with six keynote presentations. A majority of these contributions are presented by their manuscript in this collection (a few were granted to present without an accompanying manuscript).

The organizing committee would like to thank everyone who has helped with review of manuscripts, all those who helped to promote the conference and all authors who have submitted scientific contributions. We are also grateful for the support from the conference sponsors: ANSYS, SFI Metal Production and NanoSim.

Stein Tore Johansen & Jan Erik Olsen

Organizing committee:

Conference chairman: Prof. Stein Tore Johansen
Conference coordinator: Dr. Jan Erik Olsen
Dr. Bernhard Müller
Dr.Sigrid Karstad Dahl
Dr.Shahriar Amini
Dr.Ernst Meese
Dr.Josip Zoric
Dr.Jannike Solsvik
Dr.Peter Witt

Scientific committee:

Stein Tore Johansen, SINTEF/NTNU
Bernhard Müller, NTNU
Phil Schwarz, CSIRO
Akio Tomiyama, Kobe University
Hans Kuipers, Eindhoven University of Technology
Jinghai Li, Chinese Academy of Science
Markus Braun, Ansys
Simon Lo, CD-adapco
Patrick Segers, Universiteit Gent
Jiyuan Tu, RMIT
Jos Derksen, University of Aberdeen
Dmitry Eskin, Schlumberger-Doll Research
Pär Jönsson, KTH
Stefan Pirker, Johannes Kepler University
Josip Zoric, SINTEF

CONTENTS

STATE OF THE ART: MACROSCOPIC MODELLING APPROACHES FOR THE DESCRIPTION OF MULTIPHYSICS PHENOMENA WITHIN THE ELECTROSLAG REMELTING PROCESS

Christian SCHUBERT[1]*, Antje RÜCKERT[1]†, Herbert PFEIFER[1]‡

[1] RWTH Aachen University, Department for Industrial Furnaces and Heat Engineering, Kopernikusstr. 10, 52074 Aachen, GERMANY

* E-mail: schubert@iob.rwth-aachen.de
† E-mail: arueckert@iob.rwth-aachen.de
‡ E-mail: pfeifer@iob.rwth-aachen.de

ABSTRACT

The electroslag remelting (ESR) process, which is used to produce large ingots of high quality, bases on controlled solidification and chemical refinement mechanisms and is essential for the production of high quality steels and alloys designed for aeronautical, reactor chemical or nuclear applications. Due to this, it is indispensable to enable many high technological applications. Since the spreading of the industrial application of the ESR process in the 1960s, scientist and engineers worldwide are trying to deepen their understanding about this process to improve its flexibility, productivity and efficiency. Since the process conditions are very rough and measurements are quite costly, if possible at all, numerical simulation became the investigation tool of choice. Over the time, the models became more detailed and more phenomena could be taken into account. Today we are able to estimate electromagnetic fields, heat transfer, metallurgical flow and dendritic solidification in combination with each other within a macroscopic scale, based on actual physical models combined with the capabilities of numerical computing techniques. Out of this predictions about the influence of varied process control, or the occurring of macrosegregations and other defect types, became possible. In this paper state of the art, recent developments and critical aspects of the modelling of the ESR process will be shown. Common models, their strengths and weaknesses, as well as some possible approaches to presently less considered phenomena will be presented.

Keywords: Multiphase heat and mass transfer, Solidification modelling, Volume of Fluid, Electroslag remelting.

NOMENCLATURE

Greek Symbols

α	Phase fraction, [-].
ϵ	Electrical permittivity, [F/m].
λ	Heat conductivity, [W/m].
ρ	Mass density, [kg/m^3].
ϕ	Electrical potentiall, [V].
μ_D	Dynamic viscosity, [kg/(m s)].
μ	Magnetic permeability, [N/A²].
σ	Electrical conductivity, [S/m].
$\boldsymbol{\tau}$	Shear stress tensor, [Pa].

Latin Symbols

$\boldsymbol{A}$	Magnetic vector potential, [V s m^{-1}].
A_M	Mushy zone constant, [kg/(m³ s)].
$\boldsymbol{B}$	Magnetic field, [T].
$\boldsymbol{D}$	Displacement field, [C/m²].
$\boldsymbol{E}$	Electric field, [V/m].
E	Internal energy, [J].
f_l	Liquidus fraction, [-].
$\boldsymbol{F_L}$	Lorenz force, [N/m²].
$\boldsymbol{F'_L}$	Lorenz force, [N/m³].
$\boldsymbol{F'_M}$	Mushy zone damping force, [N/m³].
$\boldsymbol{F'_V}$	Volume specific force, [N/m³].
$\boldsymbol{g}$	Gravitational acceleration vector, [m/s²].
$\boldsymbol{H}$	Magnetic field intensity, [A/m].
$\boldsymbol{I}$	Identity tensor, [-].
$\boldsymbol{J}$	Electric current density, [A/m²].
K	Intrinsic permeability of a medium, [m²].
p	Pressure, [Pa].
Q_J	Joule heat, [W/m³].
Q_{LH}	Latent heat, [W/m³].
Q_S	Heat source, [W/m³].
t	Time, [s].
T	Temperature, [K].
$\boldsymbol{u}$	Velocity vector, [m/s].
ϕ	Electrical potential, [V].

Sub/superscripts

T	Transpose
eff	Effective quantities
i	Index

INTRODUCTION

The electroslag remelting respectively electroslag refining or electro-flux remelting (ESR) is a method to refine metals using a molten slag that is electrically heated up (Hoyle, 1983). It is applicable to a broad diversity of alloys and steels, for example titan- or nickel based alloys and tool steels. Hence, due to its outstanding chemical purification capabilities, it is vital for the production of certain kinds of highly stressed materials, especially those with aerospace, deep sea or reactor technology applications. Like the variety of materials and applications, several process variants based upon the ESR process exists (Nafziger, 1976, Hoyle, 1983).

In this paper, the ESR process and its common modelling methods will be described. Furthermore, we will discuss recent simulation approaches and their contribution to possible enhancements of general ESR simulations.

Process description

Figure 1 shows a schematic diagram on the advanced stage of an exemplary ESR process.
The electrode is attached to a rod by a stub, through vertical movement of the rod the electrode is immersed into the slag. With the application of an electrical current (alternating or direct current) the slag, due to its high resistance, heats up and gets molten. The electrode influenced by the slag's temperature and its immersion depth begins to melt; at the bottom of the electrode a film of molten metal collects into droplets, finally falling through the slag layer, starting to form a liquid metal pool. Due to the water cooled copper mould the liquid metal starts to solidify from outside to inside, while the liquid metal pool sustains till the process is stopped. The zone in between the liquid metal and the already solidified metal is called mushy zone. Due to solidification and cooling of the metal an air gap is formed between electrode and mould, also a solidified slag layer is brought from the slag area to the solidified metal surface (more detailed shown in Figure 3), both effects have an critical impact on the heat transfer between solidified metal and mould (as well as on electrical conduction).

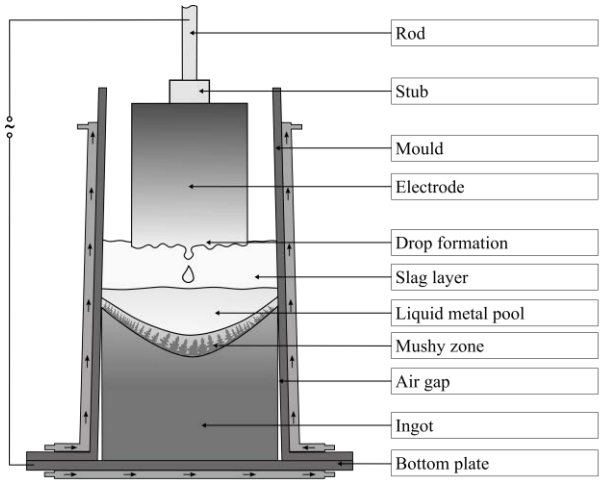

Figure 1: Schematic diagram showing an advanced stage during the ESR process.

Generally, the ESR process should reach some kind of stationary state, where the influence of the lower ingot can be neglected over the time. During these stationary phase many process parameter of the process are held constant, for example the electrode is generally controlled to hold a constant immersion depth into the slag. Due to the more or less stable conditions and its critical implication to the quality of the most of the ingot, this phase is the subject of the many ESR simulations.

MODELLING

Numerical methods became a main tool to investigate the physical behavior of remelting processes, due to the rough process conditions, which hinder detailed experimental investigations.

However caused by the many mutual coupled physical, chemical and metallurgical phenomena it is not that trivial to build a viable model, making the right simplifications, choosing adequate boundary conditions and bringing it all together using an efficient computational method. While the first ESR computational modelling approaches were mostly based on handwritten finite difference codes, for example the model of Dilawari and Szekely (1977), today modern finite volume (FV) or finite element (FE) solvers are being used.
In the following, we will describe the present, most common modelling approaches regarding the ESR process and point out various modelling challenges.
The simulated area is typically reduced to the areas described by Figure 2. Where the one zone model is probably more physical, for example including the actual behavior of the slag / liquid metal pool interface (Rückert and Pfeifer, 2009, Kharicha et al., 2010), the two zone model can be way faster, especially regarding industrial size process geometries (Giesselmann et al., 2015).

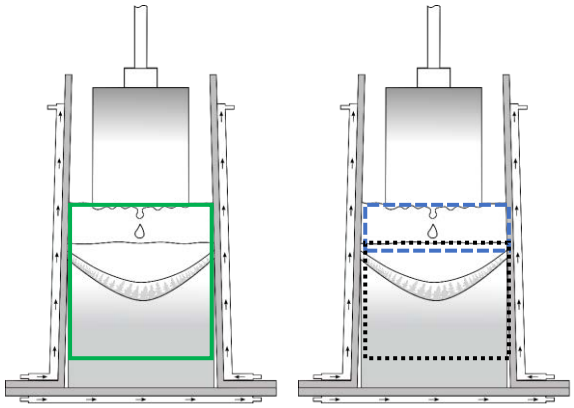

Figure 2: Common choices for computational domains within the ESR process, left side: one zone model approach and on the right side: two zone model approach

Usually a 2D axisymmetric simulation approach is used to model the ESR process, but especially in the region of the slag (see upper rectangle on the right side of Figure 2), according to Rückert (2012), Giesselmann (2014) or Karimi-Sibaki et al. (2016) this approach is only valid for the droplet behaviour in small lab scale size electrodes. It is not valid for industrial scale sized processes, as demonstrated by the non-axisymmetric dripping off behaviour, shown by the results from Kharicha et al. (2011) for full 3D models of industrial scale ESR plants. However according to Karimi-Sibaki et al. (2016) a 2D axisymmetric approach will be sufficient to model the solidification of larger ingot sizes. These findings are quite important since a 3D simulation of the whole process, speaking of real process times greater than a few seconds, will be quite unrealistic for the coming years, even utilizing the power of many core CPU clusters. So working out the right simplifications will still have a lot of impact on future simulations.

Multiphase fluid flow

The most common modelling assumption for modeling the fluid flow inside the slag and liquid metal will be shown. Therefore, the Navier-Stokes equations consisting of continuity equation (1) and momentum equation (2) for incompressible fluid flow will be used.

$$\frac{\partial \rho}{\partial t} + \nabla \cdot (\rho\, \boldsymbol{u}) = 0 \tag{1}$$

$$\frac{\partial (\rho\, \boldsymbol{u})}{\partial t} + \nabla \cdot (\rho\, \boldsymbol{u}\, \boldsymbol{u}) = -\nabla p + \nabla \cdot \boldsymbol{\tau} + \rho\, \boldsymbol{g} + \boldsymbol{F'_L} + \boldsymbol{F'_M} + \boldsymbol{F'_V} \tag{2}$$

Different volume specific force vectors account for the induced Lorentz forces, Mushy zone damping forces and other possible volume specific forces. The shear stress tensor $\boldsymbol{\tau}$ can be described according to equation (3) using the dynamic viscosity μ_D and the velocity field $\boldsymbol{u}$ (Giesselmann et al., 2015).

$$\boldsymbol{\tau} = \mu_D \left((\nabla \mathbf{u} + \nabla \mathbf{u}^{\mathrm{T}}) - \frac{2}{3} \nabla \cdot (\boldsymbol{u} \cdot \boldsymbol{I}) \right) \tag{3}$$

To describe the behavior of the liquid metal within the slag phase (see Figure 2) multiphase modelling approaches have to be used. Typically the volume of fluid (VOF) method is used for these kind of problems within FV methods (Kharicha et al., 2016, Wang et al., 2017). The VOF technique uses a single momentum equation, but solves these for each phase's volume fraction of the adapted continuity equation (4), while the sum of all volume fractions must be equal to unity as shown by equation (5).

$$\frac{1}{\rho_i} \left(\frac{\partial (\rho_i\, \alpha_i)}{\partial t} + \nabla \cdot (\rho_i\, \alpha_i\, \boldsymbol{u}) \right) = 0 \tag{4}$$

$$\sum_{i=1}^{n_{Phases}} a_i = 1 \tag{5}$$

The interface between the different phases of the VOF cells can be tracked via interface reconstruction schemes (Hyman, 1984).

Short notice on turbulence modelling

A turbulence model should be used to account for the spatially nonuniform mixing in the molten pool (Kelkar et al., 2016) or the wake flow of liquid metal droplets inside the slag area. Often the standard k-epsilon model is used for describing the turbulent phenomena in ESR flows. However, with regard to Dong et al. (2016) using the RNG k-epsilon model may be more appropriate, due to the lower Reynolds number flow. While Giesselmann et al. (2015) is using the realizable k-epsilon model. As the realizable k-epsilon model, according to the ANSYS Theory Guide (ANSYS, 2017), has shown the best performance of all the model versions for several validations studies of separated flows and flows with complex secondary flow features.
Details about the above mentioned models can be found in the ANSYS Theory Guide (ANSYS, 2017). Depending on whichever turbulence model is chosen, equation (1) to (6) may vary.

Energy equation

With the use of a RANS turbulence model the energy conservation can be described via equation (6) additionally defining the Joule heating Q_J as well as the latent heat Q_{LH}, taking care of solidification and melting heat, and possible other volumetric specific source terms Q_S.

$$\frac{\partial (\rho\, E)}{\partial t} + \nabla \cdot \left(\boldsymbol{u} \cdot (\rho\, E + p) \right) = \nabla \cdot \left(\lambda_{eff} \cdot \nabla T + \boldsymbol{\tau_{eff}} \cdot \boldsymbol{u} \right) + Q_J + Q_{LH} + Q_S \tag{6}$$

MHD equations

The electromagnetic field occurring during the ESR process can be described using the macroscopic Maxwell's equations (7)-(10), neglecting the occurrence of displacement currents ($\partial D / \partial t = 0$).

$$\nabla \times \boldsymbol{H} = \boldsymbol{J} + \frac{\partial \boldsymbol{D}}{\partial t} \tag{7}$$

$$\nabla \times \boldsymbol{E} = -\frac{\partial \boldsymbol{B}}{\partial t} \tag{8}$$

$$\nabla \cdot \boldsymbol{B} = 0 \tag{9}$$

$$\nabla \cdot \boldsymbol{D} = 0 \tag{10}$$

Furthermore, neglecting magnetization and polarization effects and assuming isotropic material behavior, the Maxwell equations can collectively be applied with the following material equations (11)-(13).

$$\boldsymbol{B} = \mu \boldsymbol{H} \tag{11}$$

$$\boldsymbol{D} = \epsilon \boldsymbol{E} \tag{12}$$

$$\boldsymbol{J} = \sigma\, (\boldsymbol{E} + \boldsymbol{u} \times \boldsymbol{B}) \tag{13}$$

Depending on the process geometry, the electrodynamic calculation should include the mold walls as well, to ensure a more accurate prediction of current flow and heat distribution in case's currents entering the mould (Kharicha et al., 2008). To describe the electrodynamic behavior various formulations can be used, for example the induction equation including various simplifications may be applied, but using the magnetic vector potential ($A - \phi$) method seems to be the method of choice regarding more complex simulations. The $A - \phi$ method states that due to equation (9) the magnetic field can be described with the rotation of an vector potential $\boldsymbol{A}$ (equation (14)). Introducing this approach leads to another degree of freedom, which can be dealt with introducing the gradient of a scalar function ϕ, which allows the electric field $\boldsymbol{E}$ to be described by equation (15).

$$\boldsymbol{B} = \nabla \times \mathbf{A} \tag{14}$$

$$\boldsymbol{E} = -\frac{\partial \boldsymbol{A}}{\partial t} - \nabla \phi \tag{15}$$

By using these equations, the Maxwell and material equations are put to one equation (16). As described by Kost (1994), the Maxwell equations can then be solved numerically utilizing a suitable gauge condition for the divergence of $\boldsymbol{A}$.

$$\nabla \times \frac{1}{\mu} \nabla \times \boldsymbol{A} + \sigma \left(\frac{\partial \boldsymbol{A}}{\partial t} + \nabla \phi \right) - \boldsymbol{u} \times \sigma \nabla \times \boldsymbol{A} = \boldsymbol{0} \quad (16)$$

Since the time step size for the calculation of changing electromagnetic fields is usually significantly smaller than the time step size used for the solution of the multiphase flow, the magnetic vector potential equation should further be simplified for stationary DC current or be solved in harmonic manner for the application of sinusoidal time varying currents.

The resulting quantities of the Lorentz force $\boldsymbol{F_L}$ used in the momentum equation as well as the Joule heating Q_J term used in the energy conservation equation can be derived using the general equations (17) and (18).

$$\boldsymbol{F_L} = \boldsymbol{J} \times \boldsymbol{B} \quad (17)$$

$$Q_J = \frac{\boldsymbol{J} \cdot \boldsymbol{J}}{\sigma} \quad (18)$$

Solidification

According to literature, a frequently used approach to model the macroscopic behavior of the solidifying metal during the ESR process is an enthalpy porosity technique introduced by Voller et al. (1990), assuming a dendritical solidification, where the interdendritic flow follows Darcy's law (equation (19)).

$$\nabla p = -\frac{\mu_D}{K} \boldsymbol{u} \quad (19)$$

Here the so called mushy zone constant A_M is used to describe the ratio between viscosity and permeability, as shown by equation (20). The function to calculate the liquids fraction f_l from the current temperature of the metal should be chosen in good agreement to the material behavior, for example the Scheil equation might be applied to various alloys.

$$\frac{\mu_D}{K} = \frac{1 - f_l}{f_l^3 + 0.001} \cdot A_M \quad (20)$$

As a result, velocity and turbulence quantities are lowered significantly in the mushy region. To determine the mushy zone constant the flow around the dendrites may be calculated, for example using the Lattice Boltzmann technique as shown by Böttger et al. (2016). However usually more simple approaches, for example the Kozeny–Carman equation, are used to approximate the permeability K over different liquidus fraction ranges (Singh et al., 2006).

MODELLING CONSIDERATIONS

Even if the general modelling approaches are quite clear regarding the main fields and phenomena occurring inside the ESR process, there are still some difficulties to deal with. In this section, we will describe some of the recent problems which emerged out of past modelling approaches.

Material data and electro chemical behavior

As often in CFD simulations appropriate material data is crucial for the calculation of plausible results. Since the thermal conditions inside the ESR process are very rough accurate measurements of density, viscosity, surface tensions and diverse electrical or thermal properties are not that easy, if possible at all. Therefore, often Computer Coupling of Phase Diagrams and Thermochemistry (CALPHAD) methods are being used to predict the high temperature material properties. Of course, using calculated material data brings another kind of uncertainty to every simulation, which generally requires some more effort in form of extensive sensitivity studies on these properties. Therefore, the research on high temperature material property measurement is an indispensable condition for the enhancement of ESR simulations.
Further problems are for example that in DC operating ESR processes the slag might undergo some electrolysis reactions, inhomogeneously influencing material properties and chemical purification reactions, but accounting for these kind of phenomena within a simulation will be quite costly speaking of modelling effort and computational expense.

Electrode melting

The actual and changing shape of the electrode during the ESR process is of high interest, because of its influence to the film thickness and the actual dropping behavior of the liquid metal, which are a main indicator for the purification potential during the process.
Karimi-Sibaki et al. (2015) have shown a first dynamic mesh based approach to model the shape of the electrode during a ESR process, but it is still missing some essential aspects already implemented into the most other ESR models.

Solidification phenomena

Due to solidification of the slag near the mold a thin slag skin layer is formed, which can be observed after the mould is removed from the ingot. This slag layer influences the heat- and electrical conductivity between mould and slag/ingot. Furthermore, with beginning of the solidification an air gap is formed between mould and ingot caused by thermal shrinkage and thermally induced stresses inside the ingot; also influencing the heat flux between ingot and mould.

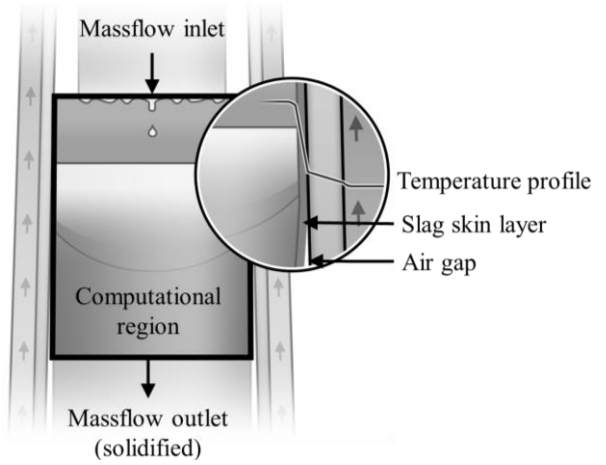

Figure 3: More detailed view of the computational region of the 1 zone model approach (Giesselmann et al., 2011) (modified)

Eickhoff et al. (2014) described an air gap developing model for the improved estimation of the air gap caused by thermally induced shrinkage, to improve the prediction of heat transfer between ingot and mould.
In many ESR simulations the slag skin is typically incorporated using a constant assumed slag skin thickness, in the best cases based on physical investigations of the represented process. Often these slag skin layer is assumed to electrically insulate the ingot area against the mould. However results of Kharicha et al. (2008), Kharicha et al. (2013) and Hugo et al. (2013) indicate that these assumption may not be right in many cases, which is essential for heat distribution and the simulated electromagnetic field and therefore probably should be context of further investigations.
Furthermore Yanke et al. (2015) incorporated the slag development of the slag skin into their ESR model, using the VOF technique, achieving quite accurate results.

Mushy zone

As mentioned in the previous section the solidification is modeled via the enthalpy-porosity approach, which can be applied assuming only dendritically solidification in the mushy zone area. Nevertheless it should be mentioned that according to Sinha et al. (1992) an anisotropic approach may be more appropriate than the isotropic approach described above in some cases.
Another problem is the that according to Giesselmann (2014) equiaxed crystal growth may occur in small sized laboratory ESR plants, in which case the aforementioned approaches are unsuitable. In the future other models available, see Wu et al. (2014), that also account for possible equiaxed crystal growth could be used.

Solidification Defects

The simulations of fluid flow, temperature and solidification are essential for understanding of the physical behavior during the ESR process. Nevertheless, the most relevant findings, at least for the industrial application of the numerical models, are the investigation or prediction of possible material defects, which might been introduced into the remolten ingot by using bad process parameters. As most solidification defects are introduced in the solidification area, for example the mushy zone, their simulative prediction strongly relies on the accurate modelling of the solidifying area. Since the methods for prediction of certain defects, for example freckles or macrosegregations, are strongly related to the used metal or alloy, they will not be further covered within this paper. Nevertheless, it is important to notice that all the results of the possible defect prediction methods depend on the aforementioned problems settings.

EXEMPLARY RESULTS

To facilitate some more insight into the process's simulation some results from the least year's research on ESR modelling at the Department for Industrial Furnaces and Heat Engineering (IOB) of the RWTH Aachen University will be shown. In Figure 4 some exemplary pictures for the slag area of a 2D axisymmetric ESR simulation are shown. The results are computed via coupling of simulations utilizing ANSYS Fluent and ANSYS EMAG. A regular sized rectangular mesh with a mesh size of around 0.5 mm is being used for the CFD and the electromagnetic simulation as well. The general simulation strategy is described in Giesselmann et al. (2011). It can be seen that the phase distribution has direct impact on the current distribution, which directly influences the joule heat generation shown in Figure 4, as you would aspect.

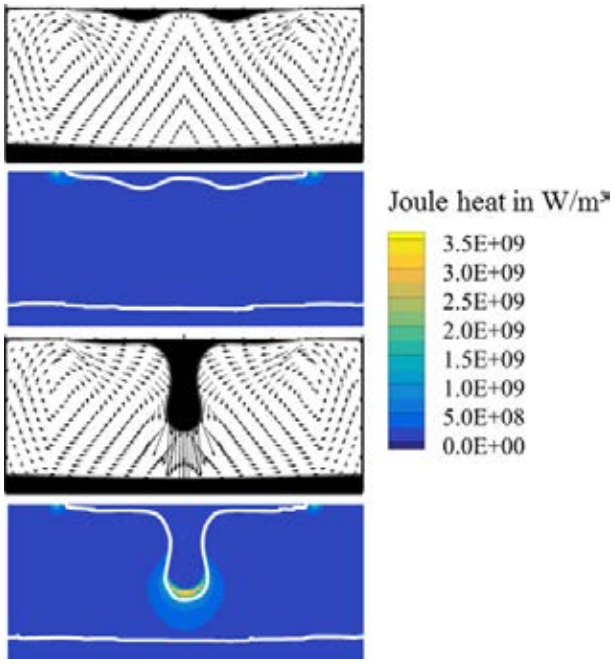

Figure 4: Exemplary view of 2D asymmetrical ESR simulation of small size ESR plant, diameter ~11 cm, metal phase is drawn in black, black line in Joule heat contour plot represents the liquid metal isosurface line, vectors representing the velocity inside the slag phase

In Figure 5 the results in the metal zone/ingot of an ESR simulation with not appropriate parametrisation can be seen. The simulation strategy of these "second zone" within a two zone modelling approach is shown in Giesselmann (2014) or Giesselmann et al. (2015).
The illustrated results (Figure 5) were generated during a parameter study investigating the impact of different slag layer heat conductivities, mushy zone constants and air gap thicknesses. Obviously, the cooling effect of the mould is excessively low in this simulation, which leads to a deep liquid metal bath, and no solidification at the

mould walls in the recirculation area. This behaviour is not expected in a real ESR process.

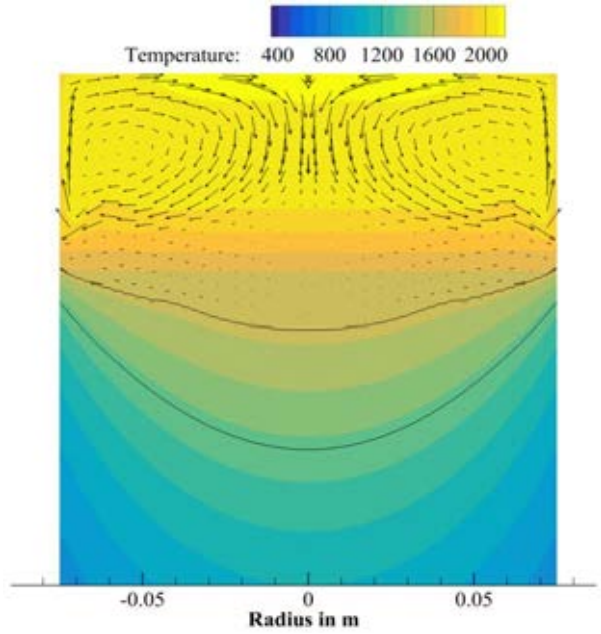

Figure 5: Contour of metal phase area of an inappropriate parametrized ESR simulation

At last, some notice should be given to the common validation method regarding ESR simulations. Since measurements at ESR plants are difficult to make during the stage of operation, typically the solidification line is determined out of the primary growth direction of the metallic grains/dendrites, extracted from prepared cross sections of a remolten ingot, as shown in Figure 6. This solidification line is taken as validation criteria by many authors.

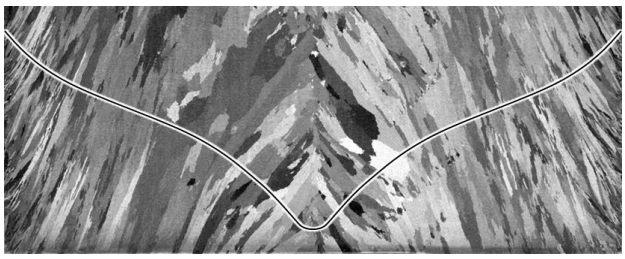

Figure 6: Cross section of etched ESR ingot with plotted solidification line (Giesselmann, 2014)

However, due to the many influencing factors to the solidification area combined with the many uncertainties in boundary conditions, material data etc., it cannot be guaranteed that a matching solidus line is sufficient to validate the whole process simulation.

CONCLUSION AND OUTLOOK

In this paper, we gave a short comprehension of the ESR process and its current modelling approaches.
Even if the general modelling strategies and necessary field equations are sufficiently elaborated at the current time. There are several insufficient investigated phenomena, whose impact on the simulation accuracy are quite uncertain, for example the slag behavior in DC operation or the changing of the shape of the electrode during the process.
Further progress could be gained by improved understanding of the processed materials properties at high temperatures, since they are also a subject of uncertainty for many simulations.
Furthermore, new experiments investigating and validating boundary conditions would improve current models, for example, heat flow measurements through the mould wall may give further conclusions about the right treatment of boundary conditions and thereby strengthen the solidus line validation criteria/method.

To sum it up, it will still need quite some time to figure out a commonly efficient and consistent solution strategy for the ESR process simulation, also including important phenomena like the electrode shape simulation, slag layer- /air gap formation, defect occurrences and accounting for relevant 3D flow phenomena. As transient full 3D simulations of the whole process will not be a feasible option during the next years, due to the required computing power.
Furthermore, this will be difficult since it should be generally possible to simulate a decent range of real process time, to allow some phenomena to actually affect the solidification area and therefore the simulated solidus line, which is an import criterion for many investigations.

At last, it should be mentioned that due to the variety of problems and phenomena in the ESR process, simulative solutions or solution approaches might also influence the research on other more or less related (metallurgical) processes.

ACKNOWLEDGMENT

The authors gratefully acknowledge the support of the German Research Foundation (Deutsche Forschungsgemeinschaft – DFG).

REFERENCES

ANSYS, INC., (2017), "ANSYS® Academic Research, Release 18.0, Help System, FLUENT Theory Guide".

BÖTTGER, B., et al., (2016), "Cross-Permeability of the Semisolid Region in Directional Solidification: A Combined Phase-Field and Lattice-Boltzmann Simulation Approach", *JOM*, **68**, 27-36.

DILAWARI, A.H. and SZEKELY, J., (1977), "A mathematical model of slag and metal flow in the ESR Process", *Metallurgical Transactions B*, **8**, 227-236.

DONG, Y.-W., et al., (2016), "Comprehensive Mathematical Model for Simulating Electroslag Remelting", *Metallurgical and Materials Transactions B*, **47**, 1475-1488.

EICKHOFF, M., et al., (2014), "Introducing an analytic approach on air gap formation during the ESR/VAR Process and numerical validation", *Ingot casting, rolling & forging : ICRF, ingot casting, rolling and forging 2014 ; 2nd International Conference ; Milan, Italy, 7 - 9 May 2014*.

GIESSELMANN, N., (2014), "Numerische Untersuchungen des Elektroschlacke-Umschmelzprozesses für Alloy 718", Dissertation, Aachen, RWTH Aachen University, Fakultät für Georessourcen und Materialtechnik, 140.

GIESSELMANN, N., et al., (2015), "Coupling of Multiple Numerical Models to Simulate Electroslag Remelting Process for Alloy 718", *ISIJ International*, **55**, 1408-1415.

GIESSELMANN, N., et al., (2011), "Mathematical modeling of the influence of process parameters on the solidification in the electroslag remelting process", "STEELSIM, International Conference Simulation and Modelling of Metallurgical Processes in Steelmaking, 4", Düsseldorf, TEMA Technologie Marketing AG, **4**.

HOYLE, G., (1983), "Electroslag processes: principles and practice", Applied Science Publishers.

HUGO, M., et al., (2013), "Impact of the Solidified Slag Skin on the Current Distribution during Electroslag Remelting", Proceedings of the 2013 International Symposium on Liquid Metal Processing and Casting, John Wiley & Sons, Inc. 79-85.

HYMAN, J.M., (1984), "Numerical methods for tracking interfaces", *Physica D: Nonlinear Phenomena*, **12**, 396-407.

KARIMI-SIBAKI, E., et al., (2015), "A Dynamic Mesh-Based Approach to Model Melting and Shape of an ESR Electrode", *Metallurgical and Materials Transactions B*, 1-13.

KARIMI-SIBAKI, E., et al., (2016), "On Validity of Axisymmetric Assumption for Modeling an Industrial Scale Electroslag Remelting Process", *Advanced engineering materials*, **18**, 224-230.

KELKAR, K.M., et al., (2016), "Computational Modeling of Electroslag Remelting (ESR) Process Used for the Production of High-Performance Alloys", Proceedings of the 2013 International Symposium on Liquid Metal Processing & Casting, M. J. M. Krane, A. Jardy, R. L. Williamson and J. J. Beaman, Cham, Springer International Publishing 3-12.

KHARICHA, A., et al., (2011), "3D Simulation of the melting during an industial scale electro-slag remelting process", *International Symposium on Liquid Metal Processing and Casting*, Nancy, France, 41-48.

KHARICHA, A., et al., (2011), "Simulation of the melting of a flat electrode during an electro-slag remelting process", *STEELSIM, International Conference Simulation and Modelling of Metallurgical Processes in Steelmaking, 4, METEC InSteelCon, 2011*, Düsseldorf.

KHARICHA, A., et al., (2010), "Influence of the slag/pool interface on the solidification in an electroslag remelting process", *Materials science forum*, 229-236.

KHARICHA, A., et al., (2008), "On the Importance of Electric Currnts Flowing directly into the Mould during an ESR Process", *steel research int.*, **Vol. 79**, 632-636.

KHARICHA, A., et al., (2013), "Contribution of the Mould Current to the Ingot Surface Quality in the Electroslag Remelting Process", Proceedings of the 2013 International Symposium on Liquid Metal Processing and Casting, John Wiley & Sons, Inc. 95-99.

KHARICHA, A., et al., (2016), "Simulation of the Electric Signal During the Formation and Departure of Droplets in the Electroslag Remelting Process", *Metallurgical and Materials Transactions B*, **47**, 1427-1434.

KOST, A., (1994), "Numerische Methoden in der Berechnung elektromagnetischer Felder", Springer-Verlag Berlin Heidelberg.

NAFZIGER, R.H., (1976), "The electroslag melting process", The electroslag melting process, U.S. Bureau of Mines.

RÜCKERT, A., (2012), "Mathematische Modellierung der Transportprozesse beim Elektroschlackeumschmelzen", Dissertation, Aachen, RWTH Aachen, Fakultät für Georessourcen und Materialtechnik, 135.

RÜCKERT, A. and PFEIFER, H., (2009), "Mathematical Modelling of the Flow Field, Temperature Distribution, Melting and Solidification in the Electroslag Remelting Process", *Magnetohydrodynamics*, **45**, 527-533.

SINGH, A.K., et al., (2006), "Role of appropriate permeability model on numerical prediction of macrosegregation", *Metallurgical and Materials Transactions B*, **37**, 799-809.

SINHA, S.K., et al., (1992), "A variable property analysis of alloy solidification using the anisotropic porous medium approach", *International Journal of Heat and Mass Transfer*, **35**, 2865-2877.

VOLLER, V.R., et al., (1990), "Modelling the mushy region in a binary alloy", *Applied Mathematical Modelling*, **14**, 320-326.

WANG, Q., et al., (2017), "A three-phase comprehensive mathematical model of desulfurization in electroslag remelting process", *Applied Thermal Engineering*, **114**, 874-886.

WU, M., et al., (2014), "Advanced Process Simulation of Solidification and Melting", *BHM Berg- und Hüttenmännische Monatshefte*, **159**, 30-40.

YANKE, J., et al., (2015), "Simulation of Slag-Skin Formation in Electroslag Remelting Using a Volume-of-Fluid Method", *Numerical Heat Transfer, Part A: Applications*, **67**, 268-292.